Functional succession of actively growing soil microorganisms during rewetting is shaped by precipitation history

Ella T. Sieradzki[1], Alex Greenlon[1], Alexa M. Nicolas[2], Mary K. Firestone[1], Jennifer Pett-Ridge[3,4], Steven J. Blazewicz[3*], Jillian F. Banfield[1,5-7*]

1 University of California Berkeley, Department of Environmental Science, Policy and Management, Berkeley CA
2 University of California Berkeley, Department of plant and microbial biology, CA, USA
3 Physical and Life Sciences Directorate, Lawrence Livermore National Laboratory, Livermore, California, USA
4 Life & Environmental Sciences Department, University of California Merced, Merced, CA, USA
5 Department of Earth and Planetary Science, University of California, Berkeley, CA, USA
6 Earth Sciences Division, Lawrence Berkeley National Laboratory, Berkeley, CA, USA
7 Chan Zuckerberg Biohub, San Francisco, CA, USA
* Corresponding authors: blazewicz1@llnl.gov and jbanfield@berkeley.edu

Keywords: soil wet-up, soil rewetting, stable isotope probing, ecophysiology, environmental microbiology, microbial ecology, metagenomics

Abstract

Background
Rewetting of seasonally dry soils induces a burst of microbial activity and carbon mineralization that changes nutrient availability and leads to taxonomic succession. Yet the microbial functions that underpin succession are not well described. Further, how previous precipitation regimes frame microbial functional capacities after rewetting and the length of time that these effects persist remain unknown. To address these questions, we performed rewetting of seasonally dry grassland soil that experienced either mean annual or reduced precipitation during the growing season using isotopically labeled water, and sampled at five time points. We used quantitative stable isotope probing (qSIP)-informed genome-resolved metagenomics to identify actively growing bacteria and archaea, to predict their traits and analyze how these traits differ over time and between precipitation treatments.

Results
We reconstructed 503 genomes representing bacteria and archaea from 11 phyla and 23 classes, of which 77 were from active organisms (15% of organisms). Actively growing organisms at any time point and in any treatment were primarily Actinobacteria, Alphaproteobacteria and Gammaproteobacteria. Growing organisms were significantly more abundant than non-growing organisms prior to the wet-up, suggesting that the traits that initiate succession are pre-defined at the end of the growing season or by survival over the dry season. Fast growing organisms had a relatively low number of carbohydrate active enzymes per genome compared to slower growing organisms. This suggests that although they are capable of degrading complex C sources such as plant material, they do not specialize in this

process. Differential abundance of carbohydrate active enzymes in growing organisms throughout the succession implies variation in substrates over time. However, nitrogen cycling pathways differed between precipitation treatments, but in growing organisms there was no change in the abundance of genes involved over time following wetup. Comparison of gene inventories prior to wet-up revealed that many genes were significantly differentially abundant between the precipitation treatments. Surprisingly, this legacy effect waned after just one week, indicating that microbial community functions likely converge early in the growing season.

Conclusions

Use of isotopic labeling of genomes of soil microorganisms during the first week after wetup revealed differences in the abundance and functional traits of actively growing organisms under two precipitation regimes. Although the legacy effect due to different rainfall inputs was short lived, it is important, given the extent of soil organic matter breakdown that occurs immediately after the first rain event in Mediterranean climates. Changes in the potential to degrade complex organic matter during the succession imply that the current paradigm that succession relies solely on labile carbon sources needs to be revisited.

Background

Following the dry season in arid and semi-arid climates, soil rewetting is a key event that triggers microbial community restructuring and substantial carbon turnover [1,2]. This sudden increase in soil moisture has a disproportionate influence on the annual carbon budget [3]. and leads to an immediate release of carbon dioxide, termed the “Birch effect”, which can arise from both abiotic and biotic processes [4–6], with biotic processes dominant in non-carbonate-rich soils [2]. Rewetting serves an extreme change for soil microorganisms forcing microbes to adapt to a new soil environment: from survival and dormancy through rapid osmotic changes that can lead to cell lysis, to peak activity within hours [7]. This change is followed by rapid community succession, with high rates of both growth and mortality that vary by taxonomic group [8]. While we understand the identities of the bacterial and archaeal taxonomic groups that respond to rewetting, the physiological traits that underpin organism interactions and enable rapid microbial growth and turnover following wet-up are poorly understood.

Prior work has investigated the organic resources available to support biogeochemical processes in soil after the first rainfall even in annual grasslands that experience a Mediterranean climate. In addition to dry plant detritus, labile carbon and nitrogen accumulate in soil over the dry season [9], in part due to low microbial metabolic rates and reduced microbial uptake of these substrates due to low microbial metabolic rates [10]. Continued activity of secreted extracellular enzymes [10,11], osmotic shock [12] and secretion of compatible solutes also contribute to the buildup of labile C and N pools [13–15]. Soil rewetting is generally followed by high degradation rates of these carbon and nitrogen substrates [16], supporting initially fast growing organisms [17]. The existing paradigm suggests these fast growers rely on labile resources. However, we know little about the growth, abundance or ,and

metabolic characteristics of initially fast growing organisms [8], which likely contribute significantly to the Birch effect.

In Mediterranean systems, climate change is predicted to cause increased water stress [18] due to decreased rainfall, extension of the dry season and increased frequency of drying/rewetting cycles, leading to more CO_2 pulses [19,20]. It has been noted that there is less immediately respirable carbon when the dry season is prolonged [10]. We hypothesized that reduced precipitation could affect the response of soil microbial communities to rewetting. Specifically, we predicted that differences in water input in the prior year would lead to differences in the sets of biogeochemical capacities of organisms that grow following wetup, and that this difference would persist into the growing season. Here, we used stable isotope-informed genome-resolved metagenomics to identify and analyze the genomes of organisms that become active in the week following soil wetup. From these genomes we predicted functional capacities of growing organisms, and investigated how these changed over time and due to differences in rainfall history. Our results reveal distinct gene inventories of fast responding organisms after wetup in soils that had experienced two rainfall treatments. We document shifts in capacities over time, consistent with changes in carbon compound resources, and convergence in the capacities of growing organisms after approximately one week.

Results

Samples of topsoil from a Mediterranean annual grassland with a reduced vs. mean precipitation experiment were collected in the late summer of 2018, prior to the first autumn rainfall event, and used for a stable isotope probing wet-up experiment with ^{18}O-water. Post addition, DNA was extracted at 6 time points (0h, 3h, 24h, 48h, 72h and 168h), density fractionated, and 5-28 Gbp of Illumina sequences were acquired per sample. 338 dereplicated metagenome assembled genomes (MAGs) were obtained from this dataset and combined with 168 MAGs from a previous metagenomic study from a nearby field site [21]. Of these, 503 genomes representing 11 phyla and 23 classes of bacteria and archaea were at least 75% complete. Three additional Firmicutes MAGs were of low quality and therefore used only for abundance and growth analyses. Of the total pool of MAGs, 199 had a breadth (covered fraction) of at least 50% in at least one sample from this study. Failure to detect the remainder of the MAGs (304/503) with coverage above this threshold may be because coverage of the genomes in any individual sample was too low to enable assembly (thus they were only reconstructed by co-assembly of data from multiple samples). However, some of these genomes were from a prior dataset sampled during winter. Sequencing reads mapped to the MAGs made up an average of 12% of total reads per unfractionated sample and 24% of reads from the density fraction samples. This level of assignment of reads to genomes is expected because the majority of DNA from soil originates from very low abundance organisms [22,23].

Atom fraction excess (AFE), a metric of growth-based activity, was calculated per MAG based on isopycnic fractionation (fractionation by ultracentrifugation due to differences in the density of the DNA resulting from heavy isotope incorporation). 79 MAGs had statistically significant isotopic enrichment in at least one time point of one watering regime, as indicated by a AFE

lower confidence interval limit > 0. This subset of organisms was considered to be growing, as isotope enrichment of DNA requires replication. Hereafter, we distinguish between analyses that include all 506 organisms and analyses of the 200 organisms that were detected by read mapping, of which 79 were growing (sup. table S1).

We used 16S rRNA based quantitative stable isotope probing (qSIP) to determine differences in post wet-up mortality in soil that experienced mean precipitation or reduced precipitation during the growing season. We also measured total soil respiration (CO_2) and new plant-derived material respiration (i.e., carbon fixed during the preceding growing season) labeled with ^{13}C. The microbial mortality rate and respiration of newly-fixed plant material were lower in the reduced precipitation treatment (p=0.08) , but total soil respiration was not significantly different between precipitation treatments (fig. 1A, B). Cumulative mortality rate was three orders of magnitude higher in the mean precipitation treatment (fig. 1C).

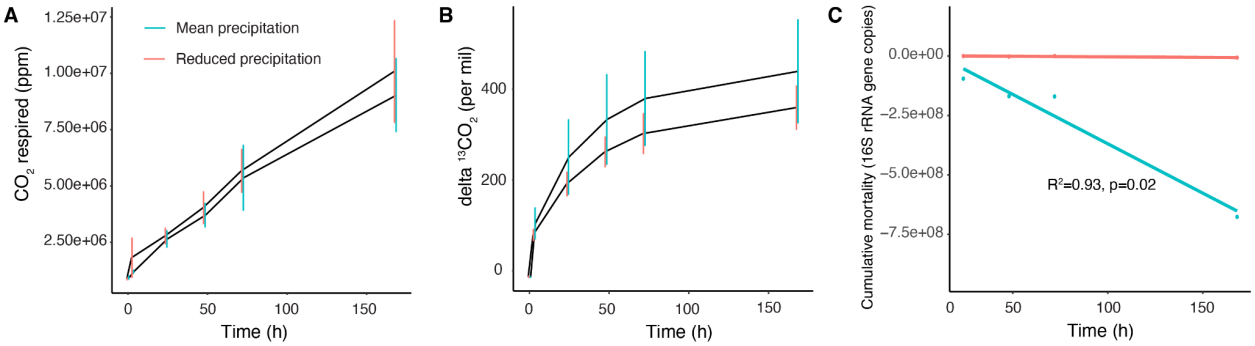

Figure 1: Comparison between precipitation treatments of (A) total soil respiration (N=3 per treatment), (B) respiration of new plant material (N=3 per treatment), (C) cumulative mortality rate starting at 24h. The linear regression of mortality in the mean precipitation treatment explained 93% of variability with p=0.02.

To test whether microorganisms classified as growing at one or more timepoints were more abundant or became more abundant compared to non-growing organisms we determined the abundance (measured as reads per kilo million, RPKM) of both growing (N=79) and non-growing (N=121) organisms at each time point and in both treatments (fig. 2). Growing microorganisms, (11.4 ± 0.5% of the community), were significantly more abundant than not growing organisms (7 ± 0.7% of the community) at time 0 for both treatments (p<0.001). There was no statistically significant change in mean abundance over the following week for growing microorganisms.

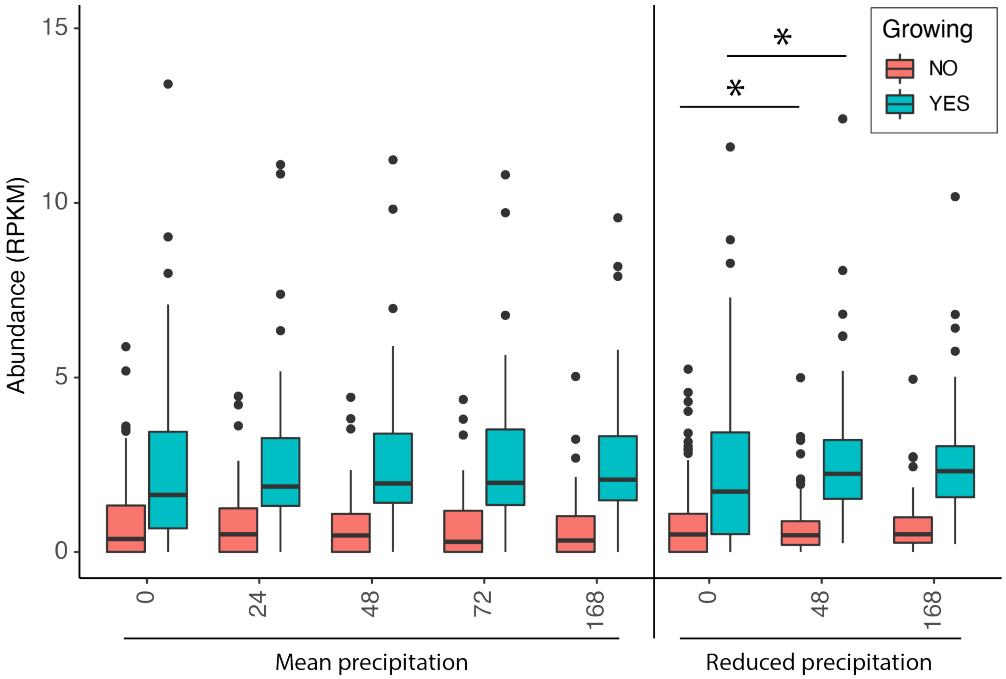

Figure 2: Organisms that were growing in the week following wet up were initially and continuously more abundant than organisms that were not growing. Abundance (RPKM) of growing organisms (N=79) vs. not growing but detected organisms (N=120) following soil wet-up after experiencing different precipitation regimes (mean or reduced) in the preceding growing season. Active organisms were identified with quantitative stable isotope probing by incorporation of ^{18}O-water. All differences between growing and not growing abundances are statistically significant ($p<0.001$), whereas trends within groups (growing or not growing) are not significant. The differences in variance (box length) between 0h and 48h in the reduced precipitation treatment are significant in both growing and not growing organisms ($p<0.05$).

To test the relationship between initial abundance and growth, we assessed whether abundant growing organisms were growing fast (AFE > 0.2) by comparing abundances and AFE values of growing microorganisms (N=79) at each time point (fig. 3). Less abundant organisms tended to be fast growing (e.g. Alphaproteobacteria and Gammaproteobacteria) whereas the more abundant organisms were slower growing (e.g., Actinobacteria) and generally remained thus. Initially abundant, albeit slow growing, organisms were mostly Actinobacteria. Significant growth was also detected in Verrucomicrobiae, Gemmatimonadetes, Chloroflexi, Myxococcia, Acidobacteria and the ammonia oxidizing archaea class Nitrososphaeria (fig. 3).

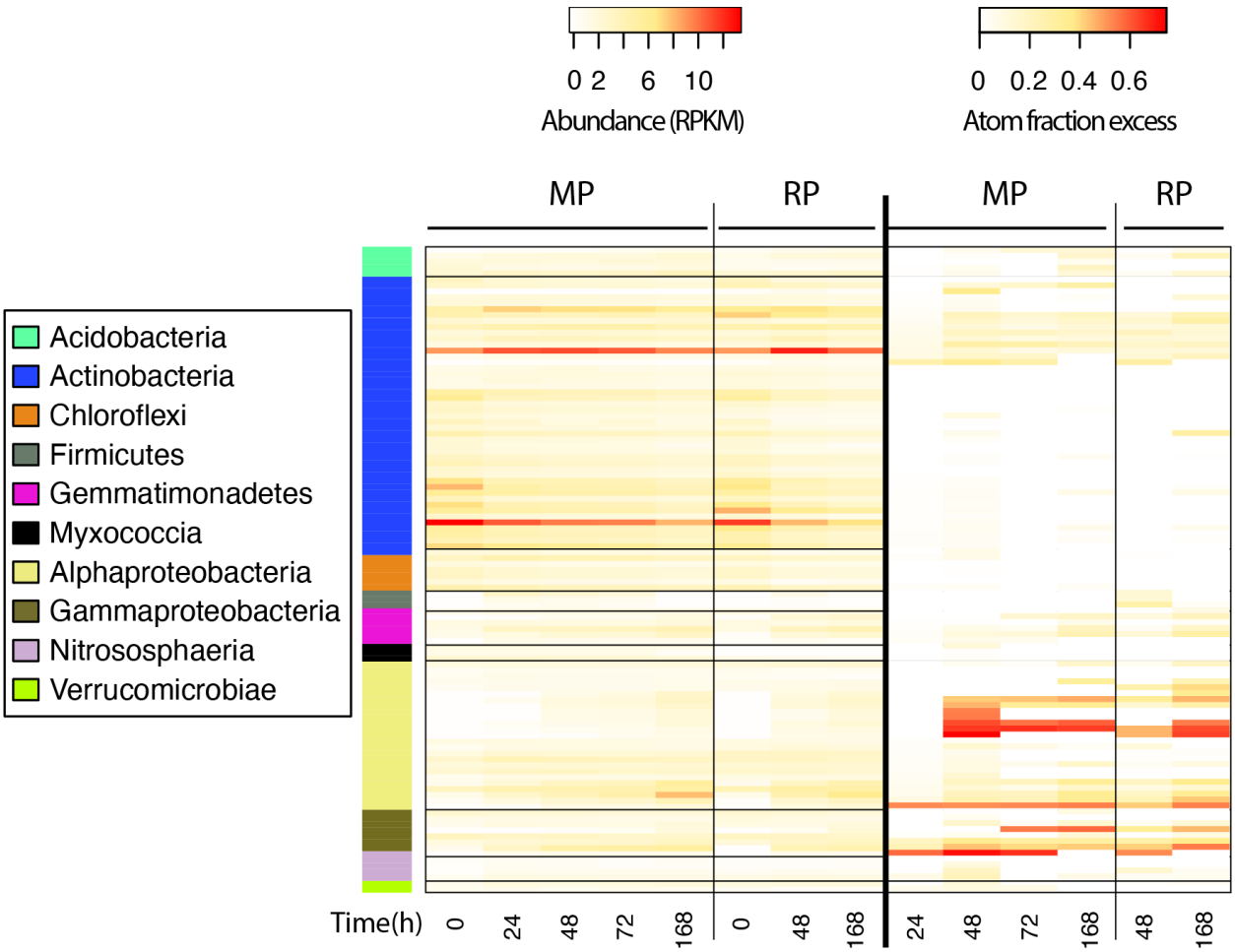

Figure 3: Abundance, enrichment and taxonomic affiliation of 79 growing taxa (atom % excess confidence interval > 0), illustrating that highly abundant organisms in both precipitation treatments were slow growing, and vice versa. Each row represents one taxon, and each column represents one time point. The heat map on the left shows abundance normalized to sample size and MAG length (RPKM) and the heat map on the right shows ^{18}O enrichment. The rows are ordered by class and enrichment within class, and the left bar represents taxonomy. MP = Mean precipitation, RP = reduced precipitation. Negative AFE values were considered undetectable and converted to zero.

Most growing organisms were isotopically enriched at multiple consecutive time points (fig. 3). To distinguish boom and bust growth dynamics compared to persistent enrichment on an organism-by-organisms basis, we plotted the number of growing organisms only at one time point vs. in multiple time points (fig. 4). A bloom of 28 newly growing organisms occurred at 48h in the mean precipitation treatment, but the majority of these organisms did not continue growing later (see leftmost column in fig. 4), representing boom and bust dynamics. In contrast, for 10 organisms, mostly Proteobacteria, we detected growth in all time points in both treatments (see rightmost column in fig. 4).

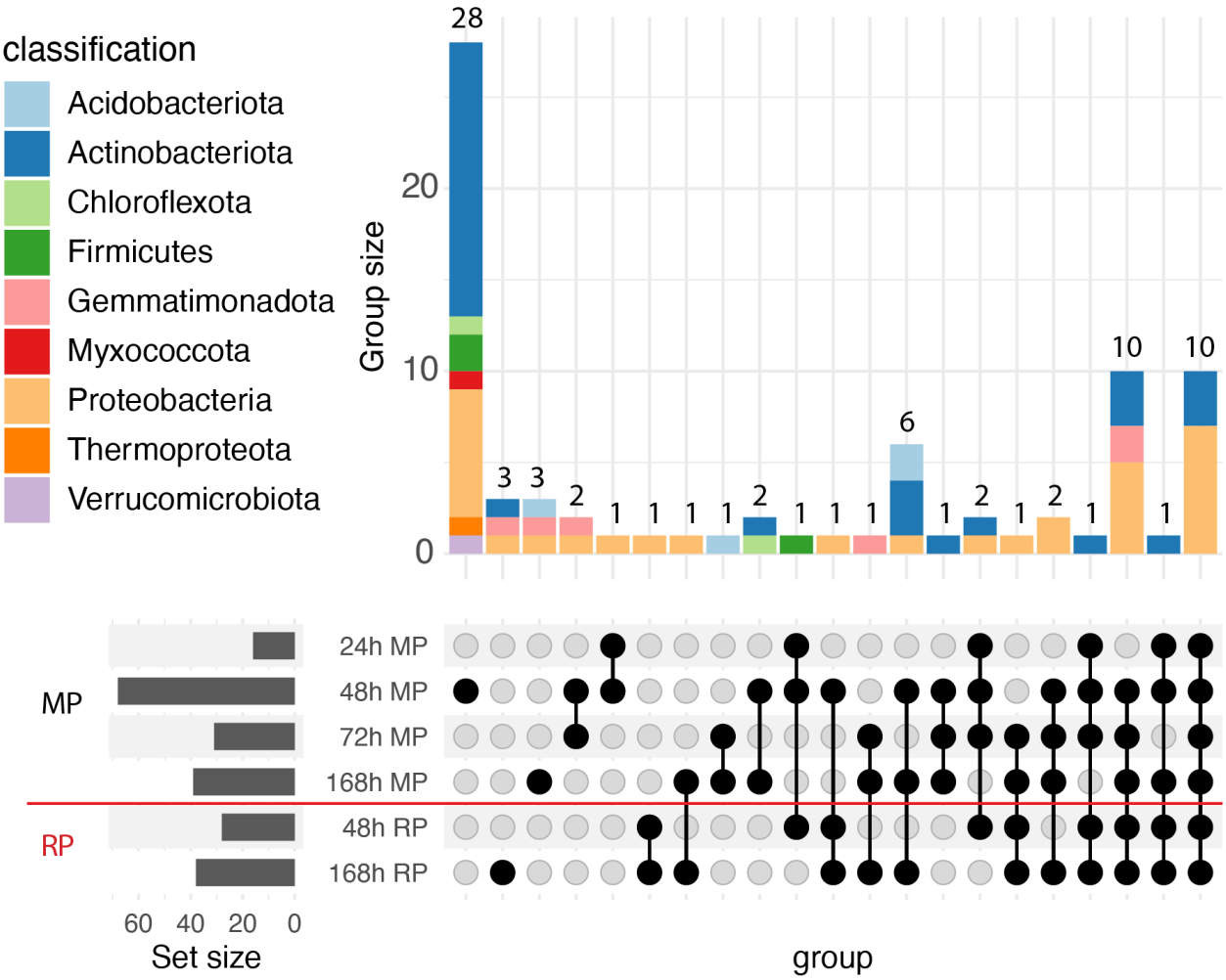

Figure 4: In both mean (MP) and reduced precipitation (RP) treatments, when grouped using growth patterns over time (black dots), it is apparent that many organisms grew in just one time point, others displayed a longer boom before bust growth pattern and some grew continuously. AFE could be calculated for 79 organisms (numbers above vertical bars). The numbers above the bars denote the number of growing organisms in a group.

To probe the extent to which changes in genetic repertoires might underpin shifts in organism abundances we compared the abundances of annotated genes in growing organisms in all samples. The purpose of this gene-centric approach was to identify genes common in growing organisms, as opposed to examining each genome of a growing organism and searching for common genes. We interpret a higher number of genes encoding a trait in growing organisms as an indication of a higher capacity of the community to perform that function. Out of 275,788 annotated genes from growing organisms (N=79), the abundance of 30,175 genes changed significantly ($p_{adj} < 0.05$), either between consecutive time points or between treatments at the same time point. In the mean precipitation treatment, the number of genes changing in abundance between consecutive time intervals varied by two to three orders of magnitude. This was not apparent in the reduced precipitation treatments (fig. 5A). However, at time 0h,

when comparing the mean vs. reduced precipitation treatments, 11,149 genes were significantly more abundant in one of the treatments (fig. 5B). Most genes at this time point were more abundant in the mean precipitation treatment (sup. fig. 1). This effect waned over time and disappeared completely at 168h (fig. 5A). Ordination of gene abundance in growing organisms revealed progressive temporal changes in community gene abundance in both precipitation treatments (fig. 5C).

An analysis of the number of differentially abundant genes over time and treatment did not differentiate between increased or decreased in abundance (fig. 5). In the mean precipitation treatment, the number of differentially abundant genes mostly decreased over the first day, became more abundant over the following day, decreased over the third day and some were more and others less abundant by the end of the week. The reduced precipitation treatment showed a distinct pattern: all differentially abundant genes were more abundant after one week. Comparing time points between treatments indicates that the majority of genes were initially more abundant in the mean precipitation compared to the reduced treatment (sup. fig. 2).

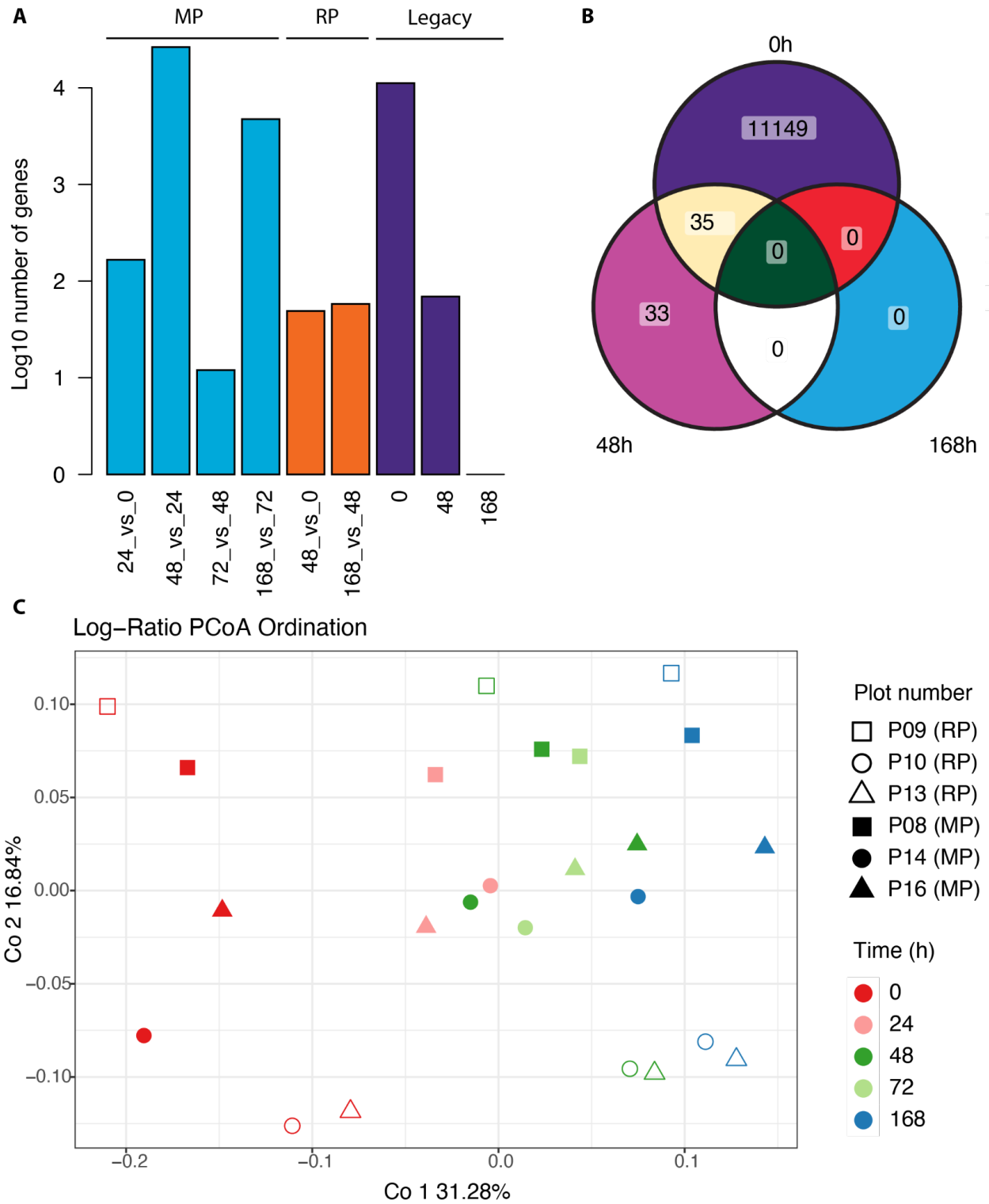

Figure 5: Changes in gene abundance over time and between precipitation treatments reflect changes in abundance of growing organisms. (**A**) Number of significantly ($p<0.05$) differentially abundant open reading frames (ORFs) at each time point compared to the previous time point (e.g. 48h vs. 24h). Three main comparisons are represented by distinct colors: Mean precipitation treatment (**MP, light blue**), Reduced precipitation treatment (**RP, purple**) and

comparison between the two at the same time point (**legacy**, **dark blue**). Note that the y axis scale is logarithmic. (**B**) Venn diagram of differentially abundant genes between MP and RP precipitation at the same time point (legacy effect). (**C**) Principal coordinates ordination of log-ratio transformed abundance of genes from growing organisms normalized to sequencing depth (N=79). Shapes represent the location of the field plot from which the metagenome was sequenced: the upper row (plots 8 and 9) or the lower row (plots 10, 13, 14 and 16; see methods). Full shapes denote MP, and empty shapes RP. The first two components explain 48% of the variance.

We tested whether any genes that changed in abundance between consecutive time intervals in a given treatment were the same. In the mean precipitation treatment, 88% of differentially abundant genes were unique to the 48h time point (sup. fig. 2A). In the reduced precipitation treatment, 99/182 differentially abundant genes were shared between 48h and 168h (sup. fig. 2B). Almost all of the genes (472/510) that differed at time 48h also differed at 0h (sup. fig. 2C).

To search for evidence of factors that may have driven changes in growth behavior over time, we evaluated inventories of genes for degradation of carbohydrates, including plant material, fungal material, and other polysaccharides. These functions are performed by carbohydrate active enzymes (CAZy). The difference in abundance pattern of CAZy genes between growing organisms (N=79) and detected but not growing organisms (N=120), i.e., which CAZy genes were more abundant than others, was significant (Wilcoxon rank sum test, $p<0.001$). Thus, organisms that grow during wet-up possess a different set of CAZy pathways compared to the rest of the bacterial and archaeal community. We looked for a correlation between the number of CAZy genes per genome and atom fraction excess, representing growth. We found that fast growing organisms (AFE>0.2, based on sup. fig. S3) generally had significantly fewer CAZy genes per genome (average 33 genes per genome), compared to an average of 41 genes per genome in slow growers (sup. fig. 3; one sided Student's t-test $p=0.02$ $t=-2$). To verify that this difference was not due to lower genome completeness of fast growing organisms, we compared these values and found no significant difference (Student's t-test, $p=0.66$).

Because degradation of complex carbohydrates happens throughout the year, we compared CAZy pathways found that in growing organisms to CAZy repertoires of the whole genomically sampled community, defined as all organisms detected in the wetup and during winter (N=503)[21]. We found degradation of rhamnose, pectin, beta mannan, mixed linkage glucans, fucose, chitin, crystalline cellulose more highly represented in growing organisms than in the total set of organisms (sup. fig. 4).

The total abundance of certain CAZy pathways, especially those related to plant material degradation, changed over time in growing organisms. When we plotted rank abundances of CAZy pathways grouped by the substrates they target (fig. 6), it is apparent for example that degradation of amorphous cellulose (C) became relatively more abundant between 24h and 48h. In contrast, xyloglucan (X) degradation became relatively less abundant between 24h and 72h. Based on the percent of growing organisms containing specific CAZy pathways, we observed a functional succession mainly of plant material degrading enzymes. These changes

were statistically significant between time points in the mean precipitation treatment, as well as between treatments after 48h, but differences between treatments were not measurable after 168h.

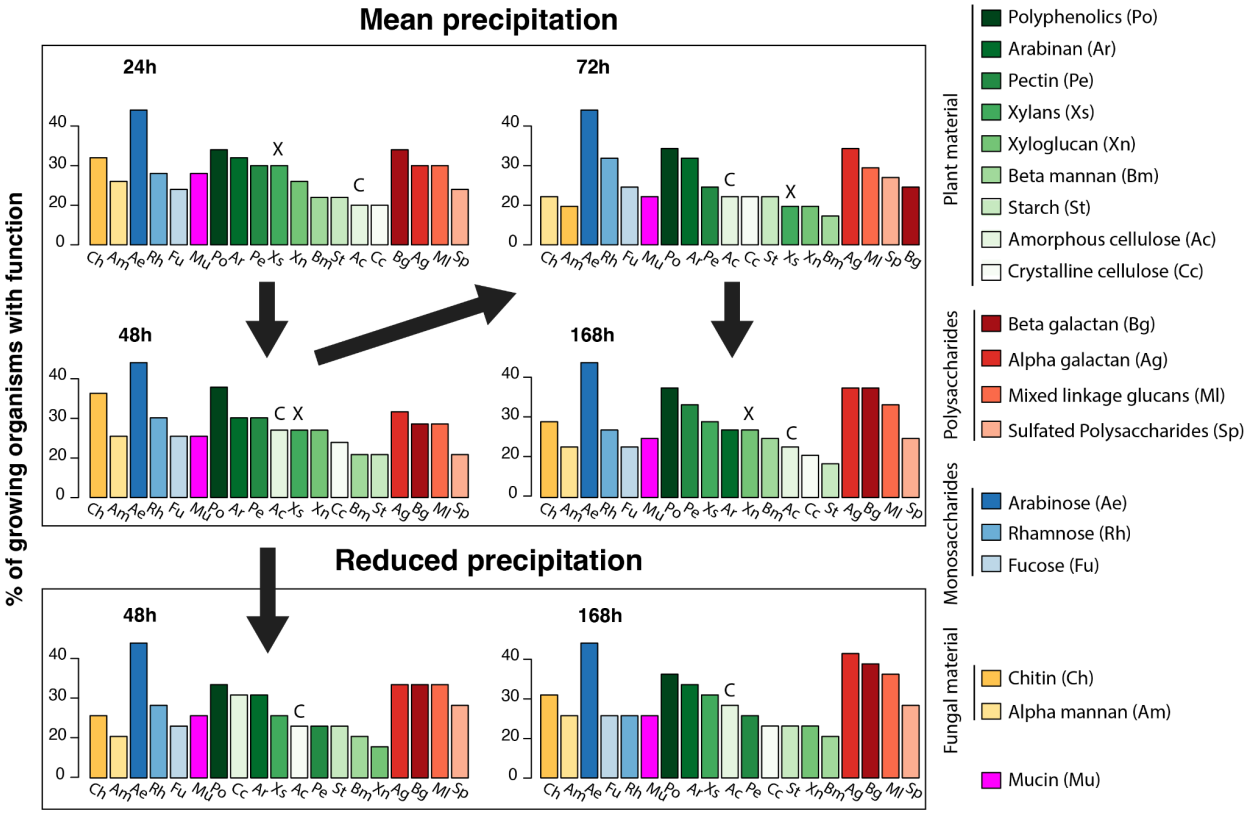

Figure 6: Percent of the organisms that were growing at each time point with genes coding for carbohydrate degradation pathways in order of time and precipitation treatment. Arrows indicate significant changes to the entire profile determined by Wilcoxon rank sum test (Benjamini-Hochberg correction for multiple comparisons $p<0.05$). Xyloglucan degradation is marked by an X and Amorphous cellulose by a C above the respective bars.

We also investigated nitrogen acquisition and cycling pathways in growing organisms. Nitrogen in soil exists mostly in the form of large, complex molecules such as proteins, chitin and nucleic acids, but it may also be present as ammonium and other inorganic nitrogen forms [24]. Some inorganic forms of nitrogen can be used as an energy source, such as oxidation of ammonium in nitrification. To determine what forms of nitrogen growing organisms were taking up or transforming during wet-up, we compared the percentage of growing organisms that contained various nitrogen related genes compared to the year-round whole community. We found enrichment of genes related to ammonium assimilation and ammonium transporters in growing organisms (fig. 7A), but no enrichment of organic nitrogen acquisition genes (fig. 7B) except for peptidases (fig. 7C). Growing organisms contained more peptidases per genome that belonged mainly to three catalytic groups: metallopeptidases, serine peptidases and cysteine peptidases (fig. 7C). While the number of peptidases per genome in growing organisms did not

change over time, there was a significant difference (p<0.05) between this number in the mean precipitation treatment at times 48 h and 72 h compared to the reduced precipitation treatment at 48 h.

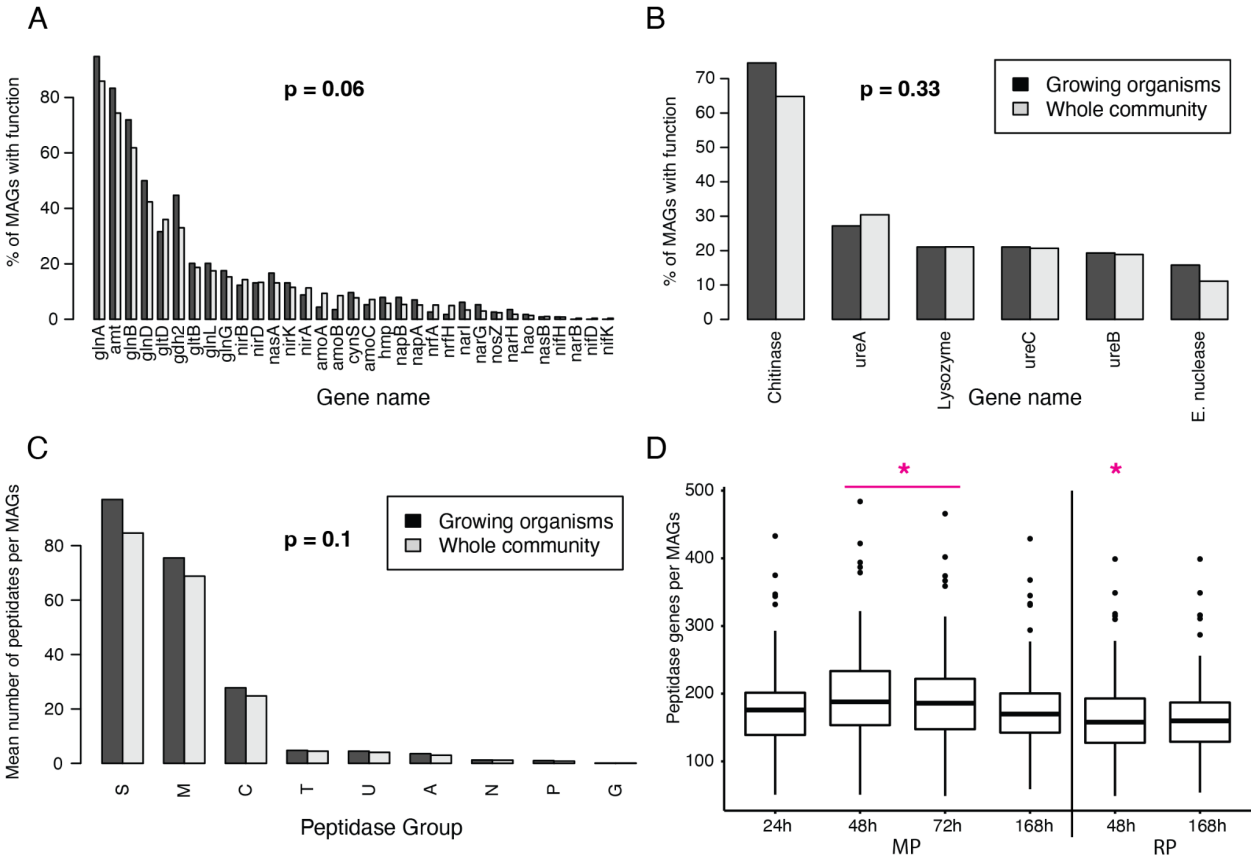

Figure 7: Presence of nitrogen acquisition and cycling traits in growing organisms. Comparison of N acquisition/cycling genes of (A) inorganic N transformations, (B) organic N transformations and (C) catalytic groups of peptidases in growing organisms vs. the whole community. P-values based on Wilcoxon rank sum test are displayed on each panel. Catalytic groups: S=serine, M=metallo, C=cysteine, T=threonine, U=unknown catalyst, A=aspartic acid, N=asparagine, =mixed, G=glutamic acid. (D) Number of peptidases per organism in growing organisms shows no significant temporal changes, but the number is significantly (p<0.05) lower at 48h in reduced precipitation compared to 48h and 72h at mean annual precipitation, indicated by pink asterisks. MP = Mean precipitation, RP = reduced precipitation

Two of the main strategies in which soil organisms can deal with dry conditions are osmolyte biosynthesis and production of extracellular polysaccharides (EPS). We searched for genes coding for biosynthesis of the osmolyte trehalose and for EPS synthesis and export. We found significantly more EPS export genes in growing organisms compared to the whole community (Student's paired t-test, p=0.003; fig. 8A) but no significant differences in trehalose synthesis (data not shown). We observed no effect of rainfall treatment or temporal changes in the percent of growing organisms that possess EPS export genes (fig. 8B). Limiting the comparison

to the five most common genes (according to fig. 7A) did not yield any significant temporal trends either.

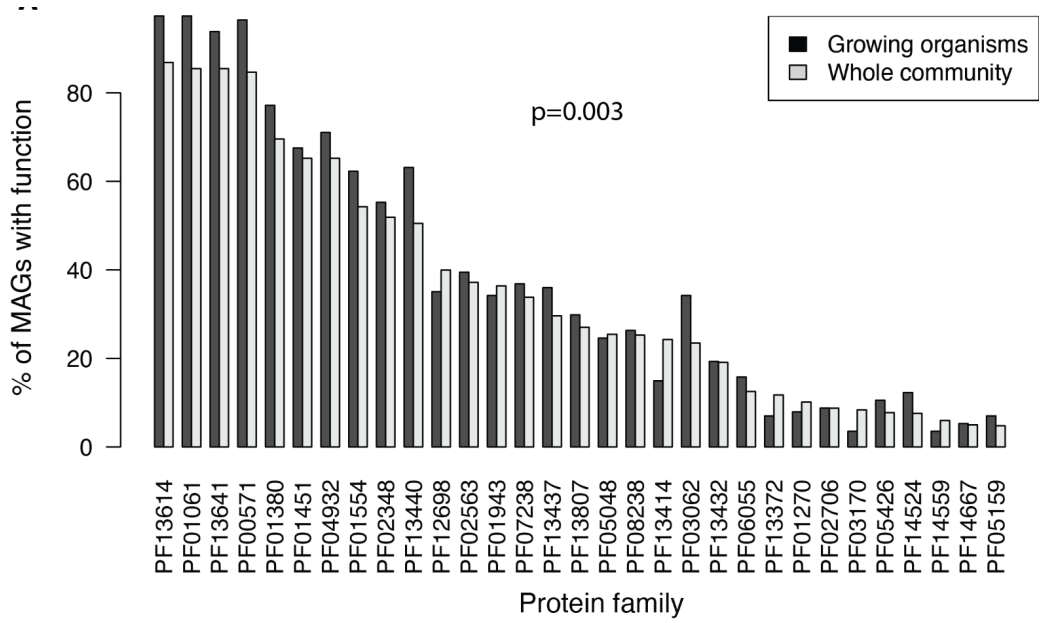

B

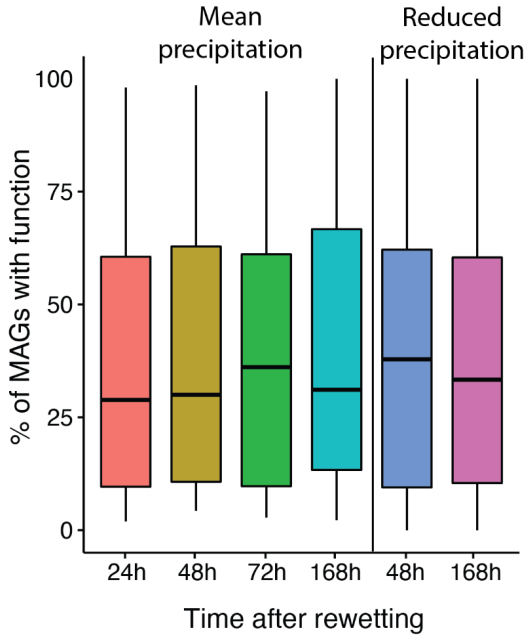

Figure 8: Presence of EPS export genes in MAGs in (A) growing organisms vs. the whole community, and (B) in growing organisms over time.

Discussion

We investigated how the history of reduced spring rainfall impacts the response of soil microbial communities to wet up and the processes by which they acquire nutrients to support growth. While climate change and its associated decrease in soil moisture are predicted to reduce grassland soil microbial diversity [25], it is the active organisms that determine ecosystem function, therefore we focused on those through stable isotope probing. Integrated results from stable isotope informed genome-resolved metagenomics, gene abundance, and gene function information enabled characterization of the traits of growing organisms that may have contributed to their proliferation during the week following rewetting. Our findings provide a mechanistic foundation for understanding of bulk rate measurements of soil biogeochemical processes following wetup (e.g., respiration; ref,). However, we acknowledge that we cannot detect growth of rare organisms due to the noise inherent in qSIP calculations. Further, at t0 a portion of soil DNA may be relic DNA (ref).

As conditions during wetup are quite distinct from those after summer drydown, we expected that organisms that were abundant during dry down would not be those that grow immediately following wet up. However, in the mean precipitation treatment, the organisms that grew over the week following wetup were a subset of those present in high abundance prior to water addition (t0). Upon wetup, growth was almost certainly primed by newly available labile compounds released by cell death [17,26]. Cell lysates may also have been available following desiccation during dry down. Thus, these organisms may simply be those that grow rapidly upon compound release following cell death.

Why were organisms that grew following wetup those that were initially more abundant? Maybe they were abundant immediately prior to dry down, or they simply survived the dry season better than others, or both. We observed a higher prevalence of genes coding for synthesis and export of extracellular polysaccharides in growing organisms compared to the whole community implying that growing organisms may be better poised to survive dry soil conditions. Thus, in combination, we suggest that organisms that were abundant at t0 and grew following wetup were those capable of surviving summer dry conditions and that can grow rapidly on cell lysates.

Of the organisms that grew, the fastest growers over the following week were the bacteria that were not the most abundant organisms. Why this is the case remains unclear, but this pattern has been observed previously in grassland soil during the winter [27].

Notably, the organisms that were least abundant prior to wetup exhibited no growth at all following water addition. We suggest that these organisms are part of the low abundance microbial “seed bank” and proliferate under conditions that differ from those studied here. Seed banks are a common strategy of microbial communities to overcome unfavorable conditions and likely underlie successional processes [28]**.**

We tracked the changes in gene abundance over the week following wetup and noted that gene abundances changed dramatically and over daily timescales. The observation that genes

in growing organisms are almost all becoming less abundant (i.e, regardless of the function of the gene) over the first 24 hr is likely attributed to community-wide mortality during the rapid change in osmotic conditions associated with rewetting of dry soil [7,8]. Reversal of this pattern over the following day is thus likely attributed to extensive growth across the community.

Organisms growing at the same time may be using similar resources, and changes in the organisms that are growing could be driven by changes in resources available. Specifically, cellular growth requires acquisition of carbon and nitrogen. The main sources of these elements in soil are organic, i.e., complex carbohydrates and large nitrogen molecules such as proteins, chitin and microbial cell walls. Therefore, we focused on the genetic repertoires related to these substrates and their differential abundances over time and between treatments.

Respiration of $^{13}CO_2$ was produced from labeled plant-derived material, likely a mixture of plant litter and microbial bodies that consumed plant material during the previous year's growing season.It has been previously suggested that in soils that experienced drought, microbes take up less plant derived ^{13}C compounds during the dry season than in soils that didn't experience drought [29]. Therefore, the slightly lower respiration of ^{13}C in the reduced precipitation treatment suggests that microbial bodies served as a carbon source following wetup. ^{13}C respiration was detected throughout the week after wetup. However, this respiration was fastest in both treatments within the first 48h, implying usage of ^{13}C-material by fast growers. Fast growing organisms had a smaller number of carbohydrate degrading enzymes than slow growers, implying that fast growth relies on labile carbon in addition to plant material. Thus, based on genetic evidence and respiration of plant-derived C, we suggest that fast growers rely not only on labile C but also on plant-derived material for growth. However, fast growers are likely better competitors for labile carbon, thus necessitating slow growers to specialize in targeting more complex carbon sources.

Importantly, the changing pattern of carbohydrate degrading enzymes over the week-long succession implies reliance on different carbohydrates. Based on succession theory, this would be linked to the changing availability of substrates, which likely drove community composition changes. In contrast, over the same time period the vast majority of growing organisms relied on the same nitrogen sources, namely ammonium and extracellular proteins. These could become available following cell death due to osmotic shock at wet-up and continued mortality during the succession. Thus, it appears that the succession we detected is driven more by carbon availability than nitrogen sources.

Our experimental strategy was designed to test for the effect of water input amount in the prior season on microbial growth and resource utilization following wetup. We refer to this as a legacy effect. One of the most striking findings of this study is the large magnitude of this effect, reflected in a difference in abundance of genes at t0 in organisms that grew after wetup. To gain insight into the causes of this legacy effect, we compared the growing microbial populations between precipitation treatments. Reduced precipitation resulted in less detectable growing organisms overall, although unlike previous studies [30] it did not result in

lower respiration. Alphaproteobacteria responded differently given their precipitation history with a delayed growth response in reduced precipitation as compared to mean annual precipitation. As field conditions were otherwise identical for both treatment groups, the explanation for the delayed response may relate to resource availability. Based on 16S rRNA qSIP, mortality after wet-up in the reduced precipitation treatment was three orders of magnitude lower than in the mean precipitation treatment. The resulting low abundance of labile carbon from cell lysis may have inhibited growth in the first two days, whereas higher mortality in the mean precipitation treatment likely supported growth. This raises the question of why lysis was less prevalent in the reduced precipitation treatment. While drying and rewetting of soil, even when they result in the same soil moisture, are very different processes [31], they both require the ability to withstand soil moisture changes. Wetup is rapid, and the organisms that survive it must be equipped to handle rapid changes in soil moisture. These same organisms would likely be those that survived faster drying due to reduced precipitation over the prior year, hence the higher abundance at t0 of organisms that grew following wetup. We suggest that an important driver of the legacy effect was the combination of bacterial resilience to osmotic stress and the resulting decrease in mortality.

In the soils that experienced reduced precipitation, the carbohydrate degradation gene sets are different compared to sets in organisms growing in soils that received mean precipitation. This may point to the availability of different carbohydrates during and after dry down between the treatment groups. Specifically, a higher fraction of the growing organisms from the reduced precipitation treatment after two days contained genes for degradation of cellulose. Thus, the capacity to degrade cellulose provided a selective advantage following wet up of soils that dried down earlier in the prior year. Further supporting this inference, increased degradation of cellulose was recently shown to be correlated to historical drought [32].

The legacy effect was surprisingly short-lived, and by the end of the week the metabolic potential of growing microorganisms that previously experienced reduced or mean precipitation converged entirely. This community “reset” could reflect convergence in resource abundance between the treatments, selecting for communities adapted to resource types historically available in this annual grassland. The implication of convergence is that as of a week after rewetting, regardless of past experiences, the microbial communities are similarly equipped for the next growing season. The intensity of drying/rewetting cycles is predicted to increase with climate change [33]. The experiment conducted here simulated this phenomenon; the results indicate that although the resistance of grassland soil communities to reduced precipitation is not high, their resilience likely is [34].

Conclusions

During wet up, a pivotal time point in soils that experience Mediterranean climates, we have some knowledge about which organisms grow, but not about which traits allow them to do so. The SIP-informed metagenomic data analysis showed that growing organisms are the ones with higher fitness during dry down and have genes for polysaccharide production and export that likely provide resistance to dessication. We report a disconnect between growth and

abundance in organisms that respond to wetup. Slow growers likely rely on complex carbon sources more than fast growers, whereas fast growers rely also on labile carbon. Finally, we demonstrate a strong but short-lived legacy effect, with convergence in the sets of growing organisms in communities that received different prior water inputs, and in their functional traits.

Methods

Field site description

This experiment used soil from the University of California Hopland Research and Extension Center (HREC) in Northern California (39° 00′ 14.6″ N, 123° 05′ 09.1″ W) on August 28th, 2018, prior to the first rainfall event. The HREC field station exists on territory originally home to the indigenous Pomo Nation. This site is characterized as having a Mediterranean climate with cool, wet winters, and hot, dry summers, and the soil belongs to the Squawrock-Witherell complex. The mean pH during fall is 7.3 with a mean C/N ratio of 10 [35].

Samples collected for this study are a subset from a larger precipitation manipulation and $^{13}CO_2$ labeling field experiment (sup. fig. 5). During the preceding two winters, the field plots were exposed to either 100% (930 mm) or 50% (465 mm) mean annual precipitation (https://hrec.ucanr.edu/Weather,_Physical,_and_Biological_Data/), and plants and exudates were isotopically labeled for 5 days in the field with $^{13}CO_2$ during the growing season (February 2018) [27,35]. During the growing season these plots were dominated by *Avena* spp. (wild oat). Labeled plants and associated soils remained intact in the field throughout the remainder of the growing season and throughout the summer dry season.

Sample collection

Topsoil cores (0-15 cm) were collected from six plots, 3 that experience mean annual precipitation and three that experiences 50%, were collected shortly before the first fall rainfall event, when average soil moisture was 3%, and transferred to the Lawrence Livermore National Laboratory where roots were picked out, and the soil samples were homogenized and sieved (2mm) to remove rocks and large plant necromass.

^{18}O-water stable isotope probing

For SIP incubations, 5 g sieved soil at mean soil moisture 1.9 ± 0.3% from each field replicate (N=3) was transferred to 15 ml Nalgene flat bottom vials. One milliliter of isotopically enriched water (98 at% ^{18}O-H_2O) or natural abundance water (as a control) was pipetted onto the soil slowly and evenly and gently mixed with the pipette tip resulting in a final average gravimetric soil moisture of 22%. After the water addition, vials were immediately sealed inside 500 ml mason jars using lids fitted with septa to facilitate headspace sampling and incubated at room temperature in the dark. Parallel jars were destructively harvested at different timepoints following wetup (0, 24, 48, 72, 168 h). At each harvest, vials containing soils were frozen in liquid nitrogen and then stored at -80°C.

DNA was extracted from all soil samples using a modified phenol chloroform protocol adapted from Barnard (2015) [36]. Three replicate extractions were conducted for each sample and then

replicate DNA extracts were combined. For each extraction, soil (0.4 g +/- 0.001) was added to 2 ml Lysing Matrix E tube (MP Biomedicals) and extracted twice as follows. 500 µl extraction buffer (5% CTAB, 0.5 M NaCl, 240 mM K_2HPO_4, pH 8.0) and 500 µl 25:24:1 phenol:chloroform:isoamyl alcohol were added before shaking (FastPrep24, MP Biomedicals: 30 s, 5.5 m s^{-1}). After centrifugation (16,100 x g, 5 min), residual phenol was removed using pre-spun 2 ml Phase Lock Gel tubes (5 Prime, Gaithersburg, MD, USA) with an equal volume of 24:1 chloroform:isoamyl alcohol, mixed and centrifuged (16,100 x g, 2 min). The aqueous phases from both extractions were pooled, mixed with 7 µl RNAase (10 mg/ml), mixed by inverting, and incubated at 50 °C for 10 min. 335 µL 7.5 M NH4+ acetate was added, mixed by inverting, incubated (4 °C, 1 h). and centrifuged (16,100 x g, 15 min. The supernatant was transferred to a new 1.7 ml tube and 1 µl Glycoblue (15 mg/ml) and 1 ml 40% PEG 6000 in 1.6 M NaCl were added, mixed by vortexing, and incubated at room temperature in the dark (2 h). After centrifugation (16,100 x g, 20 min), the pellet was rinsed with 1 ml ice-cold 70% ethanol, air-dried, resuspended in 30 µl 1xTE and stored at -80 °C.

Samples were density fractionated in a cesium chloride density gradient formed by physical density separation via ultracentrifuge as previously described with minor modifications [8]. For each sample, 5 µg of DNA in 150 µL 1xTE was mixed with 1.00 mL gradient buffer, and 4.60 mL CsCl stock (1.885 g mL^{-1}) with a final average density of 1.730 g mL^{-1}. Samples were loaded into 5.2 mL ultracentrifuge tubes and spun at 20 ºC for 108 hours at 176,284 RCF_{avg} in a Beckman Coulter Optima XE-90 ultracentrifuge using a VTi65.2 rotor. Automated sample fractionation was performed using Lawrence Livermore National Laboratory's high-throughput SIP pipeline [27,37], which automates fractionation and clean-up tasks for the density gradient SIP protocol. Ultracentrifuge tube contents were fractionated into 36 fractions (~200 µL each) using an Agilent Technologies 1260 isocratic pump delivering water at 0.25 mL min^{-1} through a 25G needle inserted through the top of the ultracentrifuge tube. Each tube was mounted in a Beckman Coulter fraction recovery system with a side port needle inserted through the bottom. The side port needle was routed to an Agilent 1260 Infinity fraction collector. Fractions were collected in 96-well deep well plates. The density of each fraction was then measured using a Reichart AR200 digital refractometer fitted with a prism covering to facilitate measurement from 5 µL, as previously described[34]. DNA in each fraction was purified and concentrated using a Hamilton Microlab Star liquid handling system programmed to automate previously described glycogen/PEG precipitations[35]. Washed DNA pellets were suspended in 40 µL of 1xTE and the DNA concentration of each fraction was quantified using a PicoGreen fluorescence assay. The fractions for each sample were binned into 5 groups based on density (1.6400-1.7039 g/ml, 1.7040-1.7169 g/ml, 1.7170-1.7299 g/ml, 1.7300-1.7449 g/ml, 1.450-1.7800 g/ml), and fractions within a binned group were combined and sequenced. Unfractionated DNA from each soil sample was also saved for sequencing.

Metagenomic analyses

Biological triplicates from three field plots of unfractionated DNA as well as DNA from 5 density fractions per sample (N=234) were sequenced using an Illumina Novaseq S4 2x150bp platform by Novogene Co. (novogene.com). Illumina adapters and phiX sequences were removed using BBmap (https://jgi.doe.gov/data-and-tools/bbtools) and the remaining reads were quality

trimmed using Sickle for paired-end reads [38]. This process yielded $155 \cdot 10^6 \pm 15 \cdot 10^6$ (mean ± standard deviation) reads per unfractionated sample, and $38 \cdot 10^6 \pm 3 \cdot 10^6$ reads per density fraction.
Triplicates of unfractionated samples from each time point were co-assembled using MEGAHIT version 1.2.9 [39] with presets large-meta and minimum contig length 1000 bp. Reads from unfractionated samples were mapped to each assembly with BBwrap requiring minimum identity 98% (https://jgi.doe.gov/data-and-tools/bbtools) and used for binning with Maxbin 2.0 [40] and MetaBAT2 [41]. Density fractions from each sample were co-assembled and binned in the same manner. Bins from each assembly were refined with the MetaWrap pipeline [42] requiring a minimum of 50% bin completion and maximum 10% bin redundancy. The resulting bins from all assemblies were dereplicated along with bins assembled from soil samples collected from a nearby site in the winter of 2018 [21] using dRep requiring 75% completeness and under 10% contamination [43] yielding 503 unique metagenome assembled genomes (MAGs): 385 from the current study and 193 from the winter study. MAG taxonomy was assigned with GTDB-tk classify workflow [44]. Three additional low quality MAGs of Firmicutes were binned manually using ggkbase. These bins were used only for SIP analyses, not for any functional analyses. We included these bins because a former 16S-rRNA qSIP analysis from the same soil [8] indicated high growth rates of Firmicutes, however we were unable to automatically assemble high quality bins of this phylum.

Reads from unfractionated samples and density fractions were mapped to the unique MAG collection as described above. Open reading frames (ORFs) were identified in MAGs with Prodigal version 2.6.3 (Hyatt et al., 2010) and annotated with DRAM [45]. Read counts per ORF from MAGs per sample were parsed with Rsubread [46] and then normalized and analyzed with DESeq2 [47].

16S rRNA gene quantification and sequencing
For 16S rRNA gene amplicon sequencing, as density fractionated DNA was amplified in triplicate 10-uL reactions using primers 515 F and 806 R [48,49]. Each reaction contained 1uL sample and 9uL of Phusion Hot Start II High Fidelity master mix (Thermo Fisher Scientific) including 1.5mM additional $MgCl_2$. PCR conditions were 95 C for 2 min followed by 20 cycles of 95 C for 30 S, 64.5 C for 30 S, and 72 C for 15 S. The triplicate PCR products were then pooled and diluted 10X and used as a template in a subsequent dual indexing reaction that used the same primers including the Illumina flowcell adaptor sequences and 8-nucleotide Golay barcodes (15 cycles identical to initial amplification conditions). Resulting amplicons were purified with AMPure XP magnetic beads (Beckman Coulter) and quantified with a PicoGreen assay on a BioTek Synergy HT plate reader. Samples were pooled at equivalent concentrations, purified with the AMPure XP beads, and quantified using the KAPA Sybr Fast qPCR kit (Kapa Biosciences). Libraries were sequenced on an Illumina MiSeq instrument at Northern Arizona University's Genetics Core Facility using a 300-cycle v2 reagent kit.

Quantitative stable isotope probing
Atom fraction excess (AFE), growth rates, mortality rates and net rates were calculated using quantitative stable isotope probing (qSIP) [8,50] by normalizing MAG relative abundance to the

quantity of DNA per density fraction [21]. Relative abundance was calculated with coverm version 0.4.0 (https://github.com/wwood/CoverM) generating read counts (method count) for MAGs with a minimum covered fraction of 50% (method covered_fraction) and dividing by total reads per sample. Cumulative mortality was calculated using mortality rates estimated with 16S rRNA gene sequence and qPCR data as described in Blazewicz et al. 2020 [8].

CO_2 Flux quantification

Headspace gas samples (5 ml) were collected at each harvest for measurements of total CO_2 and $^{13}CO_2$. with a gas-tight syringe and transferred into 20 ml wheaton serum bottles that had been purged and then filled with N_2 (1 atm). Total headspace CO_2 was quantified via gas chromotography equipped with a methanizer paired with a flame ionization detector (GC2014, Shimadzu). Carbon isotopic composition ($\boldsymbol{\delta}^{13}$C relative to the VPDB standard) of CO_2 was measured using a Picarro G2201-i cavity ring down spectrometer fitted with a small sample introduction module (SSIM).

Statistical analyses

Cumulative mortality regression was calculated with the R base function lm based on mortality values resulting from qSIP analyses.

Abundance (RPKM), read counts and breadth (fraction of MAG covered) tables of MAGs per sample were calculated with coverm (https://github.com/wwood/CoverM). For qSIP analyses, counts were converted to zero where breadth was <50%. Relative abundance was then calculated by dividing read counts per MAG by number of reads per sample. Growing organisms (N=79) were defined as MAGs with detected growth for which the lower limit of the confidence interval was greater than zero. Detected organisms (N=200) were those that had breadth >50% and RPKM >0 in at least one sample. Abundance boxplots of growing and non-growing organisms were plotted based on RPKM using ggplot2 [51].

Heatmaps for abundance and median atom fraction excess (AFE) were plotted using the R package heatmap3 [52].

Comparisons of gene abundance between time points and treatments were performed with DESeq2 [47] by defining the variable “condition” to include both time and treatment, and comparing all conditions. P values were adjusted for multiple comparisons using FDR correction.

Principal coordinates analysis was based on a Bray-Curtis dissimilarity matrix representing gene abundance per sample via the R vegan package [53], and plotted with ggplot2 [51] and ggvenn [54].

Using gene annotations from DRAM [45] we determined which MAGs of growing organisms contained CAZy pathways for degradation of carbohydrates in each time point. That number was divided by the number of growing organisms at each time point to get the percent of organisms with the capability to degrade specific substrates. The resulting table was plotted using ggplot2 [51]. Similarly, we analyzed and plotted inorganic and organic nitrogen cycling genes, as well as peptidases. Finally, we used the annotated gene abundances to search for patterns in genes coding for extracellular polysaccharide (EPS) biosynthesis and export, assuming these would be necessary to generate a biofilm.

References

1. Placella SA, Brodie EL, Firestone MK. Rainfall-induced carbon dioxide pulses result from sequential resuscitation of phylogenetically clustered microbial groups. Proc Natl Acad Sci U S A. 2012;109:10931–6.

2. Barnard RL, Blazewicz SJ, Firestone MK. Rewetting of soil: Revisiting the origin of soil CO2 emissions. Soil Biol Biochem. 2020;147:107819.

3. Xu L, Baldocchi DD, Tang J. How soil moisture, rain pulses, and growth alter the response of ecosystem respiration to temperature. Global Biogeochem Cycles [Internet]. American Geophysical Union (AGU); 2004;18. Available from: http://doi.wiley.com/10.1029/2004GB002281

4. Birch HF. The effect of soil drying on humus decomposition and nitrogen availability. Plant Soil. Martinus Nijhoff, The Hague/Kluwer Academic Publishers; 1958;10:9–31.

5. Unger S, Máguas C, Pereira JS, David TS, Werner C. The influence of precipitation pulses on soil respiration--Assessing the “Birch effect” by stable carbon isotopes. Soil Biol Biochem. Elsevier; 2010;42:1800–10.

6. Lee X, Wu H-J, Sigler J, Oishi C, Siccama T. Rapid and transient response of soil respiration to rain. Glob Chang Biol. Wiley; 2004;10:1017–26.

7. Blazewicz SJ, Schwartz E, Firestone MK. Growth and death of bacteria and fungi underlie rainfall-induced carbon dioxide pulses from seasonally dried soil. Ecology. 2014;95:1162–72.

8. Blazewicz SJ, Hungate BA, Koch BJ, Nuccio EE, Morrissey E, Brodie EL, et al. Taxon-specific microbial growth and mortality patterns reveal distinct temporal population responses to rewetting in a California grassland soil. ISME J. 2020;14:1520–32.

9. Schaeffer SM, Homyak PM, Boot CM, Roux-Michollet D, Schimel JP. Soil carbon and nitrogen dynamics throughout the summer drought in a California annual grassland. Soil Biol Biochem. 2017;115:54–62.

10. Homyak PM, Blankinship JC, Slessarev EW, Schaeffer SM, Manzoni S, Schimel JP. Effects of altered dry season length and plant inputs on soluble soil carbon. Ecology. 2018;99:2348–62.

11. Schimel J, Becerra CA, Blankinship J. Estimating decay dynamics for enzyme activities in soils from different ecosystems. Soil Biol Biochem. 2017;114:5–11.

12. Kieft TL, Soroker E, Firestone MK. Microbial biomass response to a rapid increase in water potential when dry soil is wetted [Internet]. Soil Biology and Biochemistry. 1987. p. 119–26. Available from: http://dx.doi.org/10.1016/0038-0717(87)90070-8

13. Kempf B, Bremer E. Uptake and synthesis of compatible solutes as microbial stress responses to high-osmolality environments. Arch Microbiol. 1998;170:319–30.

14. Halverson LJ, Jones TM, Firestone MK. Release of intracellular solutes by four soil bacteria exposed to dilution stress. Soil Sci Soc Am J. Wiley; 2000;64:1630–7.

15. Warren CR. Isotope pool dilution reveals rapid turnover of small quaternary ammonium compounds.

Soil Biol Biochem. 2019;131:90–9.

16. Miller AE, Schimel JP, Meixner T, Sickman JO, Melack JM. Episodic rewetting enhances carbon and nitrogen release from chaparral soils. Soil Biol Biochem. 2005;37:2195–204.

17. Hicks LC, Lin S, Rousk J. Microbial resilience to drying-rewetting is partly driven by selection for quick colonizers. Soil Biol Biochem. 2022;167:108581.

18. Lehner F, Coats S, Stocker TF, Pendergrass AG, Sanderson BM, Raible CC, et al. Projected drought risk in 1.5°C and 2°C warmer climates. Geophys Res Lett. American Geophysical Union (AGU); 2017;44:7419–28.

19. Meisner A, Rousk J, Bååth E. Prolonged drought changes the bacterial growth response to rewetting [Internet]. Soil Biology and Biochemistry. 2015. p. 314–22. Available from: http://dx.doi.org/10.1016/j.soilbio.2015.06.002

20. Meisner A, Leizeaga A, Rousk J, Bååth E. Partial drying accelerates bacterial growth recovery to rewetting. Soil Biol Biochem. 2017;112:269–76.

21. Greenlon A, Sieradzki ET, Zablocki O, Koch BJ, Foley MM, Kimbrel JA, et al. Quantitative stable-isotope probing (qSIP) with metagenomics links microbial physiology and activity to soil moisture in Mediterranean-climate grassland ecosystems [Internet]. bioRxiv. 2022 [cited 2022 May 3]. p. 2022.05.02.490339. Available from: https://www.biorxiv.org/content/10.1101/2022.05.02.490339v1

22. Pessi IS, Viitamäki S, Virkkala A-M, Eronen-Rasimus E, Delmont TO, Marushchak ME, et al. In-depth characterization of denitrifier communities across different soil ecosystems in the tundra [Internet]. bioRxiv. 2022 [cited 2022 Jun 20]. p. 2020.12.21.419267. Available from: https://www.biorxiv.org/content/10.1101/2020.12.21.419267v4

23. Xu L, Dong Z, Chiniquy D, Pierroz G, Deng S, Gao C, et al. Genome-resolved metagenomics reveals role of iron metabolism in drought-induced rhizosphere microbiome dynamics. Nat Commun. 2021;12:3209.

24. Schimel JP, Bennett J. NITROGEN MINERALIZATION: CHALLENGES OF A CHANGING PARADIGM [Internet]. Ecology. 2004. p. 591–602. Available from: http://dx.doi.org/10.1890/03-8002

25. Wu L, Zhang Y, Guo X, Ning D, Zhou X, Feng J, et al. Reduction of microbial diversity in grassland soil is driven by long-term climate warming. Nat Microbiol [Internet]. 2022; Available from: http://dx.doi.org/10.1038/s41564-022-01147-3

26. Schimel JP. Life in Dry Soils: Effects of Drought on Soil Microbial Communities and Processes. Annu Rev Ecol Evol Syst [Internet]. Annual Reviews; 2018 [cited 2022 Feb 16]; Available from: https://www.annualreviews.org/doi/abs/10.1146/annurev-ecolsys-110617-062614

27. Foley MM, Blazewicz SJ, McFarlane KJ, Greenlon A, Hayer M, Kimbrel JA, et al. Active communities and growth of soil microorganisms are framed by mean annual precipitation in three California annual grasslands [Internet]. bioRxiv. 2021 [cited 2022 Mar 27]. p. 2021.12.06.471491. Available from: https://www.biorxiv.org/content/10.1101/2021.12.06.471491v1

28. Lennon JT, Jones SE. Microbial seed banks: the ecological and evolutionary implications of dormancy.

Nat Rev Microbiol. 2011;9:119–30.

29. Fuchslueger L, Bahn M, Hasibeder R, Kienzl S, Fritz K, Schmitt M, et al. Drought history affects grassland plant and microbial carbon turnover during and after a subsequent drought event. J Ecol. 2016;104:1453–65.

30. Göransson H, Godbold DL, Jones DL, Rousk J. Bacterial growth and respiration responses upon rewetting dry forest soils: Impact of drought-legacy. Soil Biol Biochem. 2013;57:477–86.

31. Patel KF, Myers-Pigg A, Bond-Lamberty B, Fansler SJ, Norris CG, McKever SA, et al. Soil carbon dynamics during drying vs. rewetting: Importance of antecedent moisture conditions. Soil Biol Biochem. 2021;156:108165.

32. Liu L, Estiarte M, Bengtson P, Li J, Asensio D, Wallander H, et al. Drought legacies on soil respiration and microbial community in a Mediterranean forest soil under different soil moisture and carbon inputs. Geoderma. 2022;405:115425.

33. Dai A, Zhao T, Chen J. Climate Change and Drought: a Precipitation and Evaporation Perspective. Current Climate Change Reports. 2018;4:301–12.

34. Shade A, Peter H, Allison SD, Baho DL, Berga M, Bürgmann H, et al. Fundamentals of microbial community resistance and resilience. Front Microbiol. 2012;3:417.

35. Fossum C, Estera-Molina KY, Yuan M, Herman DJ, Chu-Jacoby I, Nico PS, et al. Belowground allocation and dynamics of recently fixed plant carbon in a California annual grassland. Soil Biol Biochem. 2022;165:108519.

36. Barnard RL, Osborne CA, Firestone MK. Changing precipitation pattern alters soil microbial community response to wet-up under a Mediterranean-type climate. ISME J. 2015;9:946–57.

37. Trubl G, Kimbrel JA, Liquet-Gonzalez J, Nuccio EE, Weber PK, Pett-Ridge J, et al. Active virus-host interactions at sub-freezing temperatures in Arctic peat soil. Microbiome. 2021;9:208.

38. Joshi NA, Fass J, Others. Sickle: A sliding-window, adaptive, quality-based trimming tool for FastQ files (Version 1.33)[Software]. 2011.

39. Li D, Liu C-M, Luo R, Sadakane K, Lam T-W. MEGAHIT: an ultra-fast single-node solution for large and complex metagenomics assembly via succinct de Bruijn graph. Bioinformatics. 2015;31:1674–6.

40. Wu Y-W, Simmons BA, Singer SW. MaxBin 2.0: an automated binning algorithm to recover genomes from multiple metagenomic datasets. Bioinformatics. 2016;32:605–7.

41. Kang DD, Li F, Kirton E, Thomas A, Egan R, An H, et al. MetaBAT 2: an adaptive binning algorithm for robust and efficient genome reconstruction from metagenome assemblies. PeerJ. 2019;7:e7359.

42. Uritskiy GV, DiRuggiero J, Taylor J. MetaWRAP—a flexible pipeline for genome-resolved metagenomic data analysis. Microbiome. 2018;6:158.

43. Olm MR, Brown CT, Brooks B, Banfield JF. dRep: a tool for fast and accurate genomic comparisons that enables improved genome recovery from metagenomes through de-replication. ISME J.

2017;11:2864–8.

44. Chaumeil P-A, Mussig AJ, Hugenholtz P, Parks DH. GTDB-Tk: a toolkit to classify genomes with the Genome Taxonomy Database. Bioinformatics [Internet]. 2019; Available from: http://dx.doi.org/10.1093/bioinformatics/btz848

45. Shaffer M, Borton MA, McGivern BB, Zayed AA, La Rosa SL, Solden LM, et al. DRAM for distilling microbial metabolism to automate the curation of microbiome function. Nucleic Acids Res. 2020;48:8883–900.

46. Liao Y, Smyth GK, Shi W. The R package Rsubread is easier, faster, cheaper and better for alignment and quantification of RNA sequencing reads. Nucleic Acids Res. 2019;47:e47.

47. Love MI, Huber W, Anders S. Moderated estimation of fold change and dispersion for RNA-seq data with DESeq2. Genome Biol. 2014;15:550.

48. Apprill A, McNally S, Parsons R, Weber L. Minor revision to V4 region SSU rRNA 806R gene primer greatly increases detection of SAR11 bacterioplankton. Aquat Microb Ecol. 2015;75:129–37.

49. Parada AE, Needham DM, Fuhrman JA. Every base matters: assessing small subunit rRNA primers for marine microbiomes with mock communities, time series and global field samples. Environ Microbiol. Wiley Online Library; 2016;18:1403–14.

50. Hungate BA, Mau RL, Schwartz E, Caporaso JG, Dijkstra P, van Gestel N, et al. Quantitative microbial ecology through stable isotope probing. Appl Environ Microbiol. 2015;81:7570–81.

51. Wickham H. ggplot2: Elegant Graphics for Data Analysis. Springer; 2016.

52. Zhao S, Guo Y, Sheng Q, Shyr Y. Heatmap3: an improved heatmap package with more powerful and convenient features. BMC Bioinformatics. 2014;15:P16.

53. Oksanen J, Kindt R, Legendre P, O'Hara B, Simpson GL, Solymos P, et al. The vegan package. Community ecology package [http://r-forge r-project org/projects/vegan/] [Internet]. 2008; Available from: https://www.researchgate.net/profile/Gavin_Simpson/publication/228339454_The_vegan_Package/links/0912f50be86bc29a7f000000/The-vegan-Package.pdf

54. Yan. ggvenn: Draw Venn Diagram by "ggplot2." R Package Version.

Acknowledgements

The authors thank members of the Firestone and Pett-Ridge groups who helped with field sampling and soil processing, Shufei Lei and Rohan Sachdeva for bioinformatic support, Max Li for help with the soil incubations and DNA extractions, Ryan Gini for help with GC analyses, and Marissa Lafler for operation of the LLNL qSIP pipeline and the Picarro CRDS.
This research was supported by the U.S. Department of Energy (DOE), Office of Biological and Environmental Research (BER), Genomic Science Program Lawrence Livermore National

Laboratory (LLNL) 'Microbes Persist' Soil Microbiome Scientific Focus Area SCW1632, and a subaward to UC Berkeley. Field plots and precipitation management were initially generated via DOE BER awards DE-SC0020163 and DE-SC0016247 (to MKF) and awards SCW1589, and SCW1421 (to JPR), and maintained by Dr. Mengting Yuan, Katerina Estera-Molina, and staff of the Hopland Research and Extension Center (HREC) through the University of California Division of Agriculture and Natural Resources. Work at LLNL was performed under the auspices of the DOE, Contract DE-AC52-07NA27344.

Ethics approval and consent to participate
Not applicable

Consent for publication
Not applicable

Availability of data and material
All raw data used in this publication is available on the NCBI short read archive under project submission number SUB11697222. No custom tools were used to analyze the data.

Competing interests
The authors declare that they have no competing interests.

Funding
This research was supported by the U.S. Department of Energy (DOE), Office of Biological and Environmental Research (BER), Genomic Science Program Lawrence Livermore National Laboratory (LLNL) 'Microbes Persist' Soil Microbiome Scientific Focus Area SCW1632, and a subaward to UC Berkeley. Field plots and precipitation management were initially generated via DOE BER awards DE-SC0020163 and DE-SC0016247 (to MKF) and awards SCW1589, and SCW1421 (to JPR), and maintained by Dr. Mengting Yuan, Katerina Estera-Molina, and staff of the Hopland Research and Extension Center (HREC) through the University of California Division of Agriculture and Natural Resources. Work at LLNL was performed under the auspices of the DOE, Contract DE-AC52-07NA27344.

Authors' contributions
ETS performed all bioinformatics and statistical analyses on metagenomic data, wrote and revised the manuscript.
AG provided genomic sequences used in this study, participated in sample processing and provided input on the manuscript.
AMN assisted in improving graphical illustrations and provided feedback on the manuscript.

MKF advised on paper writing and analyses and provided funding
JPR revised the paper and provided equipment, resources and funding
SJB advised on the paper, participated in writing and analyzed 16S-qSIP data
JFB advised and participated in paper writing and analyses